

Molecular modeling of Nylon 6/organoclay nanocomposite: prediction of binding energy

Maurizio Fermeglia, Marco Ferrone and Sabrina Prici

Department of Chemical Engineering – DICAMP, University of Trieste, Piazzale Europa 1, 34127 Trieste, Italy

Prepared for presentation at 2002 AIChE Annual Meeting, November 3-8, 2002, Theory, Modeling and Simulation of Nanoscale Systems II

Copyright © Maurizio Fermeglia, University of Trieste, Trieste, Italy

Unpublished

AIChE shall not be responsible for statements or opinions contained in papers or published in its publications

Abstract

In this work, we use molecular mechanics/dynamics computer simulations to predict binding energy values E_{bind} for polymer/clay nanocomposites based on nylon-6, montmorillonite and different quaternary ammonium salts. We find that E_{bind} between the polymeric matrix and the montmorillonite platelet decreases with increasing molecular volume V of the quaternary ammonium salt; contrarily, both the binding energy between the polyamide and the quat, and between the quat and the montmorillonite increase with increasing V , although with a different slope. Short aliphatic chains produce more favorable binding energies, and the presence of polar groups on the quaternary ammonium salt generally results in a greater interaction of the quat with the polymer.

Introduction

In recent years, organic-inorganic nanoscale composites have attracted great interest since they frequently exhibit unexpected hybrid properties synergistically deriving from two components. One of the most promising composite systems is the hybrids based on organic polymers and inorganic clay minerals consisting of layered silicates (PCNs).

At present, there are four principal methods for producing PCNs; of all these techniques, melt compounding is quite general, is environmentally friendly because no solvent is required, and is broadly applicable to a range of commodity polymers, from polystyrene to nylon. Nanocomposites can, therefore, be processed using currently available techniques such as extrusion, lowering the barriers towards large scale commercialization. Generally, two types of hybrid structures can be obtained upon PCN preparation: intercalated, in which a single, extended polymer chain is intercalated between the silicate layers, resulting in a well-ordered multilayer with alternating polymer/inorganic host layers, and disordered or delaminated, in which the silicate layers are exfoliated and dispersed in a continuous polymer matrix. In any case, to make a successful nanocomposite it is very important to be able to disperse the inorganic material throughout the polymer. If a uniform dispersion is not achieved, agglomerates of inorganic materials are found within the host polymer matrix, thus limiting improvement.

Similarly to polymer blends, any mixture of a polymer and layered silicate does not necessarily lead to a nanocomposite. In most, the incompatibility of the hydrophilic nature of the silicates and the hydrophobic character of most engineering polymers will induce a phase separation, similar to that of macroscopically filled systems. However, an exchange of the pristine silicate cations for alkylammonium ions both renders the clays organophilic and lowers the surface energy of the clay layers. It then becomes possible for organic species to diffuse between the layers and eventually separate them. Additionally, the alkylammonium cations can provide functional groups that can react with the polymer to improve the strength of the interface between the inorganic component and the macromolecule.

Polyamide-6 (PA-6) nanocomposites are the leader PCNs since the pioneering work performed at Toyota Central Research Laboratories in the early 80's. In the formation of nylon-6/clay nanocomposites, platelets initially stacked together to form clay particle are intercalated with the polymer, exfoliated and dispersed in the nylon matrix. In the preparation of PCNs by melt compounding, a refined smectic clay such as montmorillonite (MMT) is routinely first treated by exchanging the metal cations, residing in the interlayers, by onium ions, and in particular quaternary ammonium salts (quats). Indeed, although nylon-6 is a polar macromolecule, the driving force for nanodispersion - that is the negative change in free energy - depends on the delicate balance between the enthalpic term, due to the intermolecular interactions, and the entropic term, associated with the configurational changes in the constituents.

Therefore, because of the major role played by the clay surface modification in the thermodynamics of nanoformation, not all quats are equally effective. Indeed, some ammonium salts might result to be incompatible with the polymeric matrix, as well as some others may not be able to increase the gallery dimensions at all. Accordingly, despite the recent progress in PA-6-CN technology, there are still some fundamental questions to be answered. For instance: a) what chemistries will best exfoliate a clay in a nylon-6 matrix, and b) which of these quats are most effective in providing stronger interactions and high interfacial strength between the dispersed clay platelets and the polyamide?

In this work, we try to answer question b) by resorting to force-field based, atomistic molecular dynamics simulations for the calculation of binding energies between all PA-6-CN components. The basic machinery of the procedure consists in building a molecular model comprising nylon-6, a given quat and a MMT platelet, refining and equilibrating it by molecular mechanics/molecular dynamics, and calculating the binding energies as guidelines for screening among different quats to make nylon-6 CNs characterized by a strong interface between dispersed clay platelets and the polyamide matrix.

Computational details

A simplified model assuming all MMT platelets to be at low volume concentration and fully dispersed in the nylon-6 matrix in such a way that they do not interact consists of polyamide-6 molecules interacting with quats and exposed silicate surface on one side of a MMT clay platelet. The ammonium salts considered are reported in Table 1.

Chemical Formula	Acronym	Name
Pristine	Pristine	
$(\text{H}_3\text{C})_3\text{N}(\text{C}_6\text{H}_{13})$	M_3C_6	Trimethylhexyl quat
$(\text{H}_3\text{C})_3\text{N}(\text{C}_{12}\text{H}_{25})$	M_3C_{12}	Trimethyldodecanyl quat
$(\text{H}_3\text{C})_2\text{N}(\text{C}_{18}\text{H}_{37})_2$	$\text{M}_2(\text{C}_{18})_2$	Dimethyldistearyl quat
$(\text{H}_3\text{C})_2\text{N}(\text{C}_{18}\text{H}_{37})(\text{C}_2\text{H}_4\text{OH})$	$\text{M}_2\text{C}_{18}\text{C}_2\text{OH}$	Dimethylstearylethyleneoxide quat
$(\text{H}_3\text{C})\text{N}(\text{C}_{18}\text{H}_{37})(\text{C}_2\text{H}_4\text{OH})_2$	$\text{MC}_{18}(\text{C}_2\text{OH})_2$	Methylstearyl diethyleneoxide quat
$(\text{H}_3\text{C})_3\text{N}(\text{C}_6\text{H}_{12})\text{COOH}$	$\text{M}_3\text{C}_6\text{COOH}$	Trimethylomega-aminoanthic quat
$(\text{H}_3)\text{N}(\text{C}_{11}\text{H}_{22})\text{COOH}$	$\text{H}_3\text{C}_{11}\text{COOH}$	Omega-aminolauric acid quat

Table 1. Chemical formula, acronyms and names of quaternary ammonium salts.

The model structures of all quats were generated and subjected to an initial energy minimization using the Compass force field of Discover, the convergence criterion being set to 10^{-4} kcal/(mol Å). The conformational search was carried out using a combined molecular mechanics/molecular dynamics simulated annealing (MDSA) protocol. At the end of each annealing cycle, the structures were again energy minimized to converge below 10^{-4} kcal/(mol Å), and only the structures corresponding to the minimum energy were used for further modeling. The electrostatic charges for the geometrically optimized quat molecules were obtained by RESP, and the electrostatic potentials were produced by single-point quantum mechanical calculations at the Hartree-Fock level with a 6-31G* basis set.

Model amorphous structures for nylon-6 were generated by RIS to a DP of 24. Explicit hydrogens were used in all model systems. The relaxed structure was subjected to the same MDSA protocol applied to model the quats. At the end of each annealing cycle, the structure was again relaxed via FF. To explore a large portion of the configurational space, we used ten independent initial configurations for each nylon-6/quat system, and all energetic values reported are calculated through NVT ensemble averages of productive MD runs starting from distinctly different initial system configurations.

For the calculation of the binding energy, we considered the potential energy of the global system E_{tot} as given by the following summation:

$$E_{\text{tot}} = E^{\text{MMT}} + E^{\text{nylon-6}} + E^{\text{quat}} + E^{\text{MMT/nylon-6}} + E^{\text{MMT/quats}} + E^{\text{nylon-6/quats}} \quad (1)$$

in which the first three terms represent the energy of MMT, nylon-6 and quat (consisting of both valence and nonbonded terms), and the last three terms are the interactions energies between each of two component pairs (made up of nonbonded terms only). By definition the binding energy is the negative of the interaction energy.

The binding energy between the polymeric matrix and the mineral, the binding energies between the MMT and the quat, and between the polyamide and the quat can be calculated according to the following relationships:

$$E_{\text{bind}}^{\text{MMT/nylon-6}} = -E^{\text{MMT/nylon-6}} = -\left(E^{\text{MMT}} + E^{\text{nylon-6}} - E^{\text{MMT,nylon-6}}\right) \quad (2)$$

$$E_{\text{bind}}^{\text{MMT/quats}} = -E^{\text{MMT/quats}} = -\left(E^{\text{MMT}} + E^{\text{quats}} - E^{\text{(MMT/quats)}}\right) \quad (3)$$

$$E_{\text{bind}}^{\text{nylon-6/quats}} = -E^{\text{nylon-6/quats}} = -\left(E^{\text{nylon-6}} + E^{\text{quats}} - E^{\text{(nylon-6/quats)}}\right) \quad (4)$$

The estimation of the molecular surface areas and volumes was performed via the Connolly dot algorithm corrected to account for quantum effects.

Results and Discussion

As explained in the former section, the self- and interaction energies, followed by the binding energy, were calculated from the equilibrium conformation of the corresponding systems. These results are reported in Table 2.

From these results, three different behaviors can be observed: the binding energy between the nylon-6 and the quat decrease in an almost linear fashion with increasing quat molecular volume V ; on the other hand, $E_{\text{bind}}^{\text{nylon-6/quats}}$ and $E_{\text{bind}}^{\text{MMT/quats}}$ both increase with V , although with a different dependency (see Figure 1). Further, the highest value of the binding energy in our case corresponds to M_3C_6 , which is the quat Toyota used for the practical production of nylon-6 nanocomposites.

Since the quat molecules adsorb onto the clay surface, it may be more instructive to plot the sum of $E_{\text{bind}}^{\text{MMT/nylon-6}}$ and $E_{\text{bind}}^{\text{nylon-6/quats}}$ as a better measure of surface energy contribution. Accordingly, Figure 2 displays the dependence of this sum on V . Since the increase in $E_{\text{bind}}^{\text{nylon-6/quats}}$ with V is smoother than the decrease of $E_{\text{bind}}^{\text{MMT/nylon-6}}$ with the same quantity, the sum still decreases with increasing quat molecular volume. However, the differences in the binding energies among the different

surfactants are sensibly reduced, and smaller quats such as M_3C_6 and M_3C_6COOH have binding energy values close to the pristine MMT.

Chemical Formula	$E_{\text{bind}}^{\text{MMT/nylon-6}}$ (kcal/mol)	$E_{\text{bind}}^{\text{nylon-6/quat}}$ (kcal/mol)	$E_{\text{bind}}^{\text{MMT/quat}}$ (kcal/mol)	SA (\AA^2)	V (\AA^3)
Pristine	331				
$(H_3C)_3N(C_6H_{13})$	215.1	90.4	301.5	273.3	201.2
$(H_3C)_3N(C_{12}H_{25})$	105.3	120.5	400.9	400.9	302.8
$(H_3C)_2N(C_{18}H_{37})_2$	8.22	166.2	522.5	862.6	690.8
$(H_3C)_2N(C_{18}H_{37})(C_2H_4OH)$	21.1	144.7	470.1	556.2	429.4
$(H_3C)N(C_{18}H_{37})(C_2H_4OH)_2$	19.2	149.5	492.6	584.0	455.3
$(H_3C)_3N(C_6H_{12})COOH$	172.8	96.4	344.7	296.3	226.7
$(H)_3N(C_{11}H_{22})COOH$	119.1	111.9	388.1	363.8	275.8

Table 2. Binding energies calculated from simulation according to eqns. (3)-(5), and molecular areas and volumes of the quats.

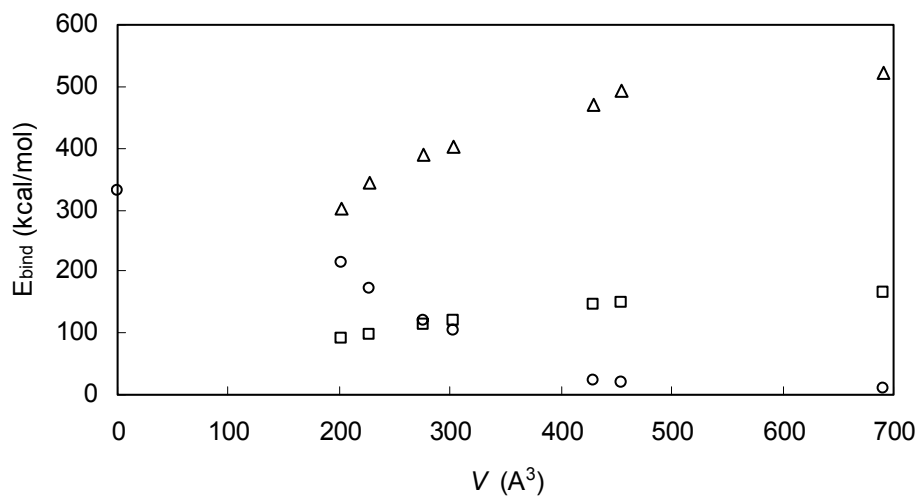


Figure 1. Predicted E_{bind} vs. quat molecular volume V . (○), $E_{\text{bind}}^{\text{MMT/nylon-6}}$; (□), $E_{\text{bind}}^{\text{nylon-6/quat}}$; (Δ), $E_{\text{bind}}^{\text{MMT/quat}}$.

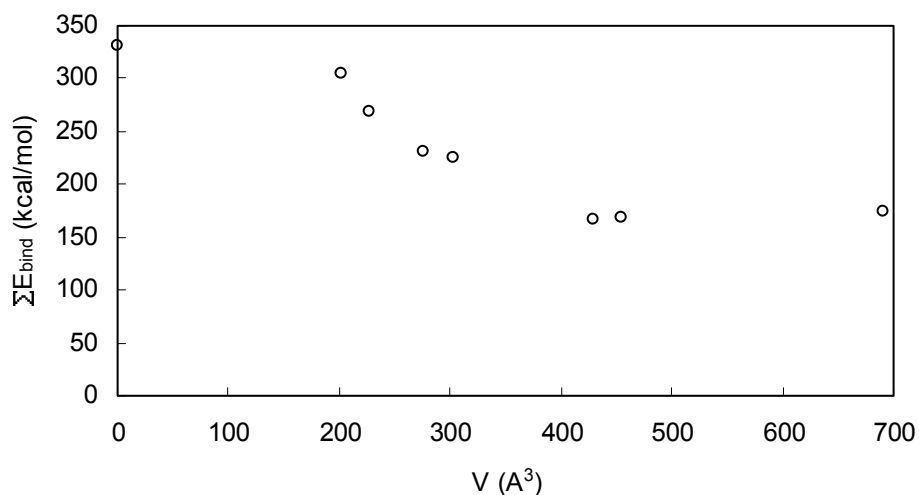


Figure 2. Sum of $E_{\text{bind}}^{\text{MMT/nylon-6}}$ and $E_{\text{bind}}^{\text{nylon-6/quat}}$ vs. quat molecular volume V .

Conclusions

By applying atomistic molecular simulation to PCNs composed by MMT, nylon-6 and different quats, we found that the energy of binding between the polymeric matrix and the montmorillonite platelet shows a decreasing trend with increasing molecular volume V of the quaternary ammonium salt used as surfactant. At the same time, both the binding energy between the polyamide and the quat, and between the quat and the montmorillonite increase with increasing V , although with a different slope. Short aliphatic chains are more effective in producing favorable binding energies, and the presence of polar groups on the quaternary ammonium salt generally results in a greater interaction of the quat with the polymer.

Acknowledgments

Authors wish to thank the Italian Ministry for University and Scientific and Technological Research (MURST, Rome, Italy) for special grant (PRIN 2001).